

# Long-term Phase-coherent X-ray Timing of PSR B0540–69

Margaret A. Livingstone<sup>1</sup>, Victoria M. Kaspi, Fotis P. Gavriil

*Department of Physics, Rutherford Physics Building, McGill University, 3600 University Street, Montreal, Quebec, H3A 2T8, Canada*

## ABSTRACT

We present a new phase-coherent timing analysis for the young, energetic pulsar PSR B0540–69 using 7.6 yr of data from the *Rossi X-Ray Timing Explorer*. We measure the braking index,  $n = 2.140 \pm 0.009$ , and discuss our measurement in the context of other discordant values reported in the literature. We present an improved source position from the phase-coherent timing of the pulsar, to our knowledge, the first of its kind from X-ray pulsar timing. In addition, we detect evidence for a glitch which has been previously reported but later disputed. The glitch occurred at MJD  $51335 \pm 12$  with  $\Delta\nu/\nu = (1.4 \pm 0.2) \times 10^{-9}$  and  $\Delta\dot{\nu}/\dot{\nu} = (1.33 \pm 0.02) \times 10^{-4}$ . We calculate that the glitch activity parameter for PSR B0540–69 is two orders of magnitude smaller than that of the Crab pulsar which has otherwise very similar properties. This suggests that neutron stars of similar apparent ages, rotation properties and inferred dipolar B fields can have significantly different internal properties.

*Subject headings:* pulsars: general—pulsars: individual (PSR B0540–69)—X-rays: stars

## 1. Introduction

Young, rotation-powered pulsars spin down sufficiently rapidly to provide interesting tests of the simple model of pulsar spin down, given by

$$\dot{\nu} = -K\nu^n, \quad (1)$$

where  $\nu$  is the spin frequency,  $\dot{\nu}$  is the frequency derivative, and  $K$  is a constant related to the magnetic field, moment of inertia, and angle between the spin and magnetic axes. The

---

<sup>1</sup>maggie@physics.mcgill.ca

braking index,  $n$ , is equal to 3 for magnetic dipole radiation in a vacuum. A measurement of the second frequency derivative,  $\ddot{\nu}$ , allows for the calculation of  $n$ . Measurements of  $n$  give crucial insight into the electrodynamics of pulsars. Only five such measurements have been made (Lyne et al. 1993, 1996; Deeter et al. 1999; Camilo et al. 2000; Livingstone et al. 2005). Interestingly, all of these values are less than 3 and span a relatively wide range:  $n = 1.4 \pm 0.2$  to  $n = 2.91 \pm 0.05$ . The physical implications of  $n < 3$  are still debated; possible explanations include the removal of angular momentum by a pulsar wind (Manchester & Peterson 1989) and a time-dependent magnetic field (Blandford & Romani 1988).

Some pulsars, especially the youngest ones, exhibit significant deviations from the standard spin-down model. Two types of deviations are known, timing noise – a low-frequency random process of unknown physical origin superposed on the deterministic spin-down of the pulsar – and glitches, sudden increases in rotation rate likely caused by catastrophic unpinning of superfluid vortices (e.g. Lyne & Smith 1990).

One of the objects for which  $n$  has been reported,  $\sim 1500$  yr old PSR B0540–69, has had several contradictory values quoted in the literature. The measured values were obtained from timing observations made using a variety of instruments operating from radio frequencies into the X-ray energy range and have produced values that range from  $n = 1.81 \pm 0.07$  to  $2.74 \pm 0.10$  (Zhang et al. 2001; Ögelman & Hasinger 1990). The differences among the measured values clearly signal contamination by one or more of timing noise, unidentified glitches, or even pulse counting errors.

In this paper, we re-examine 4.6 yr of data from the *Rossi X-ray Timing Explorer* (*RXTE*) reported on by Zhang et al. (2001) and Cusumano et al. (2003) who arrived at contradictory conclusions. We also extend the data set to a total of 7.6 yr. We present a measurement of  $n$  for PSR B0540–69 with a partially phase-coherent analysis, and confirm it by performing a fully phase coherent analysis. We show that there is indeed evidence for a glitch near MJD  $51335 \pm 12$  as reported by Zhang et al. (2001), but disputed by Cusumano et al. (2003). However, we show that the correct value of  $n$  is  $2.140 \pm 0.009$ , within  $2\sigma$  of that reported by Cusumano et al. (2003).

## 2. Observations

Observations of PSR B0540–69 were obtained using the Proportional Counter Array (PCA; Jahoda et al. 1996) on board *RXTE*. The PCA consists of an array of five collimated xenon/methane multi-anode proportional counter units (PCUs) operating in the 2 – 60 keV range, with a total effective area of approximately  $6500 \text{ cm}^2$  and a field of

view of  $\sim 1^\circ$  FWHM. We used 7.6 yr of public archival *RXTE* observations collected in “GoodXenon” mode, which records the arrival time (with  $1\text{-}\mu\text{s}$  resolution) and energy (256 channel resolution) of every unrejected event. We used all layers of each PCU in the 2–18 keV range. A similar energy range was used by both Zhang et al. (2001) and Cusumano et al. (2003), as it maximizes the signal-to-noise ratio for this source. Because PSR B0540–69 was most often not the primary target of *RXTE* in these observations, integration times range from  $\sim 1$  to  $>10$  ks, resulting in a variety of signal-to-noise ratios for individual pulse profiles.

The observations were reduced using standard FITS tools as well as specialized software developed independently. Data from the different PCUs were merged and binned at  $1/1024$  ms resolution. The data were then reduced to barycentric dynamical time (TDB) at the solar system barycenter using, at first, a position determined by *Chandra* observations (Kaaret et al. 2001) and the JPL DE200 solar system ephemeris. Once a timing solution was determined, we were able to fit for the position of the pulsar, as explained in §3.3. We then re-barycentered the data at the best-fit timing position. Each time series was folded with 32 phase bins using the ephemeris obtained by Deeter et al. (1999), as this ephemeris produced the highest quality pulse profiles. Resulting profiles were cross-correlated in the Fourier domain with a high signal-to-noise ratio template created by adding phase-aligned profiles from all observations. We implemented a Fourier domain filter by using the first 6 harmonics in the cross-correlation, appropriate for this broad pulse profile. The cross-correlation produces an average time of arrival (TOA) for each observation with typical uncertainty 0.75 ms. TOAs were fitted to a timing model (see §3) using the pulsar timing software package TEMPO <sup>1</sup>.

### 3. Phase-Coherent Timing Analysis

To determine spin parameters for PSR B0540–69, we phase-connected 7.6 yr of timing data, that is, accounted for each turn of the pulsar. This is achieved by fitting TOAs to a Taylor expansion of pulse phase,  $\phi$ . At time,  $t$ ,  $\phi$  can be expressed as:

$$\phi(t) = \phi(t_0) + \nu_0(t - t_0) + \frac{1}{2}\dot{\nu}_0(t - t_0)^2 + \frac{1}{6}\ddot{\nu}_0(t - t_0)^3 + \dots, \quad (2)$$

where the subscript 0 denotes a parameter evaluated at the reference epoch,  $t_0$ . TOAs and initial parameters are input into TEMPO, which gives as output refined spin parameters and residuals. To determine an approximate input ephemeris, we performed a periodogram analysis on 5 observations from MJD 51197 - 51206. This provided 5 values for  $\nu$ , on which

---

<sup>1</sup>[www.atnf.csiro.au/research/pulsar/tempo](http://www.atnf.csiro.au/research/pulsar/tempo)

we performed a least-squares fit, resulting in an initial estimate for  $\dot{\nu}$ . We then applied the center value of  $\nu$  and the fit value of  $\dot{\nu}$  to the phase data and ‘bootstrapped’ a more accurate ephemeris which we extended over long time spans.

We performed two timing analyses on the data. In §3.1, we describe our partially phase-coherent analysis, which determined spin parameters while minimizing the effects of timing noise and covariances arising from a polynomial fit to the data. In §3.2 we describe our fully phase-coherent timing analysis, done to confirm our partially coherent results and examine the timing noise apparent in the data. §3.3 describes a position fit performed using phase-coherent timing.

### 3.1. Partially phase-coherent timing analysis

The traditional method of phase-connecting all available data has resulted in many important pulsar timing results owing to the accuracy available with absolute pulse numbering. However, in cases where timing noise seriously contaminates the data, many higher-order frequency derivatives are required to satisfactorily fit the data by removing red noise. This invariably introduces serious covariances between the fit spin parameters, without entirely removing the contamination from the timing noise.

A partially phase-coherent analysis is less sensitive to contamination from timing noise. In this method, we phase-connect subsets of the data, where the length of each subset is determined by it being the longest that requires only  $\nu$  and  $\dot{\nu}$  be fit while having residuals consistent with white noise. In this way, the 7.6 yr of data were divided into 22 subsets. The measured values of  $\dot{\nu}$  in these subsets are shown in Figure 1. A discontinuity can clearly be seen in this plot. We interpret it as a glitch that occurred at  $\text{MJD } 51342 \pm 24$ , where the epoch is taken to be the midpoint between the two neighbouring measurements, and the uncertainty is the range between these values. In §3.2 we confirm this interpretation using the more traditional fully coherent fit. A more accurate glitch epoch is impossible to ascertain from the partially coherent method due to sparse sampling and the small magnitude of the glitch.

A value for  $\ddot{\nu}$  obtained from the slope of the best-fit line to all of the data will clearly be different from that obtained in two separate fits of the pre- and post-glitch data. The pre-glitch value of  $\ddot{\nu}$  implies  $n = 2.135 \pm 0.016$ , while the post-glitch value yields  $n = 2.144 \pm 0.007$ , where the uncertainties are obtained by a bootstrap analysis which gives accurate uncertainties in cases where the formal uncertainties are thought to underestimate the true values, i.e. in the presence of timing noise (Efron 1979). The two values of  $n$  are

in agreement within the quoted uncertainties; thus we quote the average of the pre- and post-glitch values,  $n = 2.140 \pm 0.009$ .

Figure 2 shows the measurements of  $\dot{\nu}$  with the pre-glitch slope fitted out. This plot clearly shows the change in  $\dot{\nu}$  at the epoch of the glitch. The change in  $\Delta\dot{\nu}/\dot{\nu}$  is  $\sim (1.5 \pm 0.1) \times 10^{-4}$ . The significant trend in the post-glitch data in Figure 2 can be readily explained by timing noise.

By further subdividing the data, we measured 38 values for  $\nu$ . Fitting the pre-glitch trend ( $\dot{\nu}$  and  $\ddot{\nu}$ ) and removing it from the data shows the influence of the glitch on  $\nu$  as presented in Figure 3. No jump in  $\nu$  can be seen at the glitch epoch owing to the small magnitude of the glitch (as shown in §3.2). In fact,  $\Delta\nu$  is on the same order as the uncertainty in the frequency measurements, rendering the partially phase-coherent method unsuitable for measuring a meaningful  $\Delta\nu/\nu$  in this case. Spin and glitch parameters obtained in the partially coherent analysis are given in Table 1.

### 3.2. Fully Phase-Coherent Timing Analysis

To confirm the result obtained with the partially coherent timing analysis and obtain more precise glitch parameters, we phase connected all 7.6 yr of timing data. We first connected the data without allowing for a glitch in order to see if one was required by the fit. No phase jump was apparent at the epoch of the reported glitch, MJD 51325, however, we found that the timing residuals grew very significantly when connecting over this epoch. In order to phase connect the full data set with frequency derivatives and no glitch,  $\nu$  and 11 frequency derivatives were required, as shown in Figure 4, resulting in  $n = 1.968 \pm 0.004$ .

We then allowed for a glitch near the epoch of that reported by Zhang et al. (2001). In this case, the data can be fit well with 3 glitch parameters (epoch,  $\Delta\nu$ , and  $\Delta\dot{\nu}$ ) and 3 spin parameters ( $\nu$ ,  $\dot{\nu}$ , and  $\ddot{\nu}$ ). Residuals for this fit are shown in the top panel of Figure 5. The best fit glitch parameters, as determined with TEMPO, gives a glitch epoch of MJD  $51335 \pm 12$ , in agreement with the partially phase-coherent analysis.

We found  $\Delta\nu/\nu = (1.4 \pm 0.2) \times 10^{-9}$ , which was undetectable in the partially coherent analysis, and  $2.5\sigma$  from the value reported by Zhang et al. (2001). We also found  $\Delta\dot{\nu}/\dot{\nu} = (1.33 \pm 0.02) \times 10^{-4}$ , in agreement with the partially coherent analysis, but  $10\sigma$  larger than that reported by Zhang et al. (2001),  $\Delta\dot{\nu}/\dot{\nu} = (0.85 \pm 0.05) \times 10^{-4}$ .

To conclusively show that the model with the glitch is a better description of the data, we fitted additional frequency derivatives until the same number of parameters was included

in each fit (i.e. 12 parameters). The bottom panel of Figure 5 shows the results of this fit. Note that the RMS residual is a factor of 5.15 smaller for the model with the glitch, corresponding to a reduced  $\chi^2$  of 1.86 for 545 degrees of freedom, compared to a reduced  $\chi^2$  of 49.4 for 545 degrees of freedom for the fit with no glitch. This confirms the conclusion of our partially coherent analysis, namely that a glitch occurred as reported by Zhang et al. (2001).

The phase-connected solution with the minimum number of derivatives (i.e. the number required to obtain phase-connection, in this case, 2), and the glitch fitted, gives a value of  $n = 2.10657 \pm 0.00001$ . However, since there is clearly low-frequency noise contaminating the data (top panel of Figure 5), the formal uncertainty greatly underestimates the true uncertainty on  $n$ . Spin parameters vary when higher order derivatives are fitted due both to timing noise and covariances between parameters (Livingstone et al. 2005). Thus, we estimate the upper limit on the uncertainty in  $n$ , albeit not rigorously, from the variation in the measured value as higher order derivatives are added to the fit. This method implies an uncertainty of  $2.11 \pm 0.06$ , in agreement with the value obtained in the partially phase-coherent analysis. All spin and glitch parameters from the fully phase-coherent analysis are given in Table 1. Uncertainties given for parameters are the formal uncertainties, except in the case of  $n$ .

### 3.3. Timing Position

Our initial timing analysis was first performed using the pulsar position determined in a *Chandra* observation (Kaaret et al. 2001). The reported  $1\sigma$  uncertainty was  $0.7''$  on the *Chandra* position. Holding this position fixed, the post-fit residuals for the fully phase-coherent analysis showed periodic behaviour, with a period of 1 year and amplitude  $\sim 5$  ms, shown in the top panel of Figure 6 (which also has fitted the glitch and 8 frequency derivatives as in Figure 5). This suggested a small but highly significant position hence barycentering error. We found that the periodicity in the residuals changes negligibly when higher order derivatives are fitted, implying that a polynomial does not describe the trend in the data. We performed a grid search for position by re-barycentering the data and calculating TOAs for each new position. We then phase-connected each set of new TOAs and calculated post-fit residuals. We found that the position that minimizes the RMS residuals is RA= $05^{\text{h}}40^{\text{m}}11^{\text{s}}.16 \pm 0^{\text{s}}.04$  and Dec= $-69^{\circ}19'53''.9 \pm 0''.2, 1''.3$  from the *Chandra* position. The phase-coherent RMS residuals fall by a factor of  $\sim 2$  and the reduced  $\chi^2$  is smaller by a factor of 4 when the fitted position is used. More importantly, the periodic trend in the data is removed by this fit, shown in the bottom panel of Figure 6. Remaining

systematics are likely due to timing noise. All quoted parameters for the phase-coherent and partially phase-coherent analysis are calculated using the new position. However, none of the spin parameters is significantly different from what is obtained using the *Chandra* position. To our knowledge, this is the first time phase-coherent X-ray timing has been used to try to improve a source position. If correct, we have effectively demonstrated superior source localization using the non-imaging, 1°-FOV PCA compared with that attainable with *Chandra*. However, it is possible that the source timing noise is merely mimicking a position error; continued timing will confirm or refute this result.

## 4. Discussion

### 4.1. The Braking Index

By performing both a phase-coherent and a partially phase-coherent analysis on 7.6 yr of timing data for PSR B0540–69, we have found  $n = 2.140 \pm 0.009$ . This value, stationary across the glitch epoch, is similar to that reported by Deeter et al. (1999),  $n = 2.080 \pm 0.003$  based on five years of GINGA data, and  $1.7\sigma$  from that obtained by Cusumano et al. (2003),  $n = 2.125 \pm 0.001$ , based on 4.6 yr of *RXTE* data. Cusumano et al. (2003) however, reported no glitch and their uncertainty on  $n$  does not account for the effects of timing noise. The reason for the good agreement between our measured values is that despite the fact that they report no glitch, the value given for  $n$  is obtained from phase-coherent fits to the data before and after the glitch reported by Zhang et al. (2001), instead of a fit to all 4.6 yr as would be appropriate if no glitch had occurred. We phase connect the same 4.6 yr of data they used without a glitch and find  $n = 1.73 \pm 0.03$ , significantly different from the value obtained not considering the glitch, further implying the occurrence of a glitch.

Our value of  $n$  is significantly larger than that reported by Zhang et al. (2001),  $n = 1.81 \pm 0.07$ . We find that if we phase-connect only the same 300-day data set they used, we obtain a value  $n = 1.82 \pm 0.01$ , in agreement with their result. Thus their measurement was clearly contaminated by timing noise and/or glitch recovery, and affected by the relatively small time baseline used to measure  $n$ .

The value of  $n = 2.140 \pm 0.009$  is significantly less than that for simple magnetic dipole radiation,  $n = 3$ . In fact, all measurements of  $n$  thus far are less than 3. Several explanations for this have been proposed. Loss of angular momentum owing to a particle wind (which young pulsars are well known to have) could account for this (Manchester & Peterson 1989). Another explanation is that the neutron star loses additional rotational energy by torquing a disk of supernova fallback material (Menou et al. 2001). Another explanation is a time-

varying magnetic field (Blandford & Romani 1988). The presence of a time-varying magnetic field can be determined by measuring a value of the third frequency derivative larger or smaller than that predicted by the spin-down model. The simple spin-down model given in Equation 1 assumes a constant value of  $K$ , which is only valid if the magnetic field, moment of inertia, and angle between the spin and magnetic axes are all constant. With present data, the third frequency derivative is not measurable for PSR B0540–69 because of contamination from timing noise. It is possible that, as observations continue, this parameter will be measurable. For both the Crab pulsar and PSR B1509–58, values of  $\ddot{\nu}$  have been measured and are consistent with the spin-down law (Lyne et al. 1993; Livingstone et al. 2005).

## 4.2. Glitches and Timing Noise

We found that the best description of the 7.6 yr of *RXTE* data include a glitch at MJD  $51335 \pm 12$ . Our partially phase-coherent analysis shows a clear discontinuity in  $\dot{\nu}$  (Figures 1 and 2). The fully phase coherent analysis confirms this result. This glitch was previously reported by Zhang et al. (2001), at MJD  $51325 \pm 45$  and later refuted by Cusumano et al. (2003), who claimed that the data could be described by fitting higher order derivatives, that is, timing noise. The detected glitch has a small magnitude in both  $\Delta\nu/\nu$  and  $\Delta\dot{\nu}/\dot{\nu}$  which Cusumano et al. (2003) cite as evidence that no glitch occurred. However, fitting derivatives to the data shows that the residuals increase dramatically when fitting over the epoch of the reported glitch. This is exactly what is expected from a glitch, and is not expected from timing noise, which increases residuals gradually as observations are added. In addition, the partially coherent analysis shows a clear discontinuity in  $\dot{\nu}$  near (within uncertainties) the epoch of the glitch found by the phase-coherent analysis (Figure 5). Sparse observations of this source previous to the *RXTE* timing program most likely would not have been able to distinguish a small glitch from timing noise. Undetected glitches of the same magnitude as the one reported here are a likely explanation of the wide range of reported values of  $n$ .

Although the magnitude of the glitch is small, it is similar to the smallest glitches experienced by the Crab pulsar, which is close in age, spin-down luminosity ( $\dot{E} = -4\pi^2 I \nu \dot{\nu}$ ), and dipole magnetic field ( $B_0 \sim 3.3 \times 10^{19} (P\dot{P})^{1/2}$ ) to PSR B0540–69. In fact, PSR B0540–69 is often referred to as the “Crab Twin” due to these similarities. The Crab pulsar has glitched with parameters as small as  $\Delta\nu/\nu \sim 2 \times 10^{-9}$  and  $\Delta\dot{\nu}/\dot{\nu} \sim 10^{-5}$  (Lyne et al. 1993). However, the Crab pulsar also experiences glitches on the order of  $\Delta\nu/\nu \sim 10^{-8}$  with values of  $\Delta\dot{\nu}/\dot{\nu}$  as large as  $4 \times 10^{-4}$  (Wang et al. 2001). None of these larger magnitude glitches has been observed in PSR B0540–69.



The glitch activity parameter,  $A_g$ , is defined as the cumulative change in frequency from all glitches over the observation length,  $A_g = \Sigma(\Delta\nu/\nu)/\Delta t$  (McKenna & Lyne 1990). The Crab pulsar has been observed to glitch 14 times between 1969 and 2000 and has a glitch activity parameter  $A_g \simeq 0.1 \times 10^{-7} \text{ yr}^{-1}$  (e.g. Shemar & Lyne 1996). PSR J1119–6127, aged  $\sim 1600$  yr with a measured braking index,  $n = 2.91 \pm 0.05$  has been observed to glitch once implying  $A_g \simeq 0.02 \times 10^{-7} \text{ yr}^{-1}$  (Camilo et al. 2000). However, the fact that PSR J1119–6127 glitched during less than 2 yr of observations implies that this pulsar likely glitches often and may prove to have a glitch activity parameter on the order of that of the Crab pulsar, or larger. At the opposite end of the spectrum lies the  $\sim 1700$  year old pulsar PSR B1509–58, which has not glitched in 21.3 yr of observations (Livingstone et al. 2005).

The single observed glitch in PSR B0540–69 between 1996 and 2004 implies  $A_g \sim 0.002 \times 10^{-7} \text{ yr}^{-1}$ . Undetected glitches occurring in the period prior to *RXTE* observations would increase  $A_g$  and could be the source of discrepant values of  $n$  in the literature. However, it is also possible that the pulsar did not glitch during this time period, which would lower the overall value of  $A_g$ . In this case, the range of reported values of  $n$  would be due to timing noise and/or pulse counting errors. The sparse nature of observations (and in some cases data quality) between 1979 and 1996 precludes conclusions on this point. Although the estimate of  $A_g$  is based on a single glitch and is therefore extremely sensitive to any future glitch activity, it is clear that PSR B0540–69 glitches less than the Crab pulsar and somewhat more than PSR B1509–58. Thus, there is a range of possible glitch activity amongst very young pulsars.

The variety of glitch activity is suggestive of a range of internal temperatures among young pulsars, since glitch activity is possibly associated with neutron-star temperature (McKenna & Lyne 1990). In this theory, the very young pulsars such as the Crab, PSR J1119–6127, PSR B1509–58 and PSR B0540–69 have small glitch activities because they are relatively hot. Pulsars that are slightly older, e.g. the 10-kyr old Vela pulsar, are cooler and have larger glitch activities,  $\sim 8 \times 10^{-7} \text{ yr}^{-1}$  (Dodson et al. 2002, and references therein). Finally, as pulsars become much older and cooler, they are believed to eventually stop glitching entirely. However, recent reports of glitches in AXPs, which are thought to be hot neutron stars, argues that temperature is not the only factor in determining glitch behaviour (Kaspi et al. 2000; Kaspi & Gavriil 2003; Dall’Osso et al. 2003). Regardless, it is intriguing that there is such a wide variety of glitch behavior in young pulsars.

This research made use of data obtained from the High Energy Astrophysics Science Archive Research Center Online Service, provided by the NASA-Goddard Space Flight Center. VMK is a Canada Research Chair and an NSERC Steacie Fellow. Funding for this work was provided by NSERC Discovery Grant Rgpin 228738-03 and Steacie Supplement

Smfsu 268264-03. Additional funding came from Fonds de Recherche de la Nature et des Technologies du Quebec (NATEQ), the Canadian Institute for Advanced Research, and the Canada Foundation for Innovation.

## REFERENCES

- Blandford, R. D. & Romani, R. W. 1988, MNRAS, 234, 57P
- Camilo, F., Kaspi, V. M., Lyne, A. G., Manchester, R. N., Bell, J. F., D’Amico, N., McKay, N. P. F., & Crawford, F. 2000, ApJ, 541, 367
- Cusumano, G., Massaro, E., & Mineo, T. 2003, A&A, 402, 647
- Dall’Osso, S., Israel, G. L., Stella, L., Possenti, A., & Perozzi, E. 2003, ApJ, 599, 485
- Deeter, J. E., Nagase, F., & Boynton, P. E. 1999, ApJ, 512, 300
- Dodson, R. G., McCulloch, P. M., & Lewis, D. R. 2002, ApJ, 564, L85
- Efron, B. 1979, The Annals of Statistics, 7, 1
- Jahoda, K., Swank, J. H., Giles, A. B., Stark, M. J., Strohmayer, T., Zhang, W., & Morgan, E. H. 1996, Proc. SPIE, 2808, 59
- Kaaret, P., Marshall, H. L., Aldcroft, T. L., Graessle, D. E., Karovska, M., Murray, S. S., Rots, A. H., Schulz, N. S., & Seward, F. D. 2001, ApJ, 546, 1159
- Kaspi, V. M. & Gavriil, F. P. 2003, ApJ, 596, L71
- Kaspi, V. M., Lackey, J. R., & Chakrabarty, D. 2000, ApJ, 537, L31
- Livingstone, M. A., Kaspi, V. M., Gavriil, F. P., & Manchester, R. N. 2005, ApJ, 619, 1
- Lyne, A. G., Pritchard, R. S., Graham-Smith, F., & Camilo, F. 1996, Nature, 381, 497
- Lyne, A. G., Pritchard, R. S., & Smith, F. G. 1993, MNRAS, 265, 1003
- Lyne, A. G. & Smith, F. G. 1990, Pulsar Astronomy (Cambridge: Cambridge University Press)
- Manchester, R. N. & Peterson, B. A. 1989, ApJ, 342, L23
- McKenna, J. & Lyne, A. G. 1990, Nature, 343, 349
- Menou, K., Perna, R., & Hernquist, L. 2001, ApJ, 559, 1032
- Ögelman, H. & Hasinger, G. 1990, ApJ, 353, L21
- Shemar, S. L. & Lyne, A. G. 1996, MNRAS, 282, 677

Wang, N., Wu, X. J., Manchester, R., Zhang, J., Lyne, A. G., & Yusup, A. 2001, *Chin. J. Astron. Astrophys.*, 1, 195

Zhang, W., Marshall, F. E., Gotthelf, E. V., Middleditch, J., & Wang, Q. D. 2001, *ApJ*, 554, L177

Table 1. Parameters for PSR B0540–69.

| Parameters for timing analysis                           |  |
|--|--|
| Dates (Modified Julian Day)                              | 50150 – 52935  |
| Right Ascension <sup>a</sup> (J2000)                     | 05 <sup>h</sup> 40 <sup>m</sup> 11 <sup>s</sup> .16 ± 0 <sup>s</sup> .04 |
| Declination <sup>a</sup> (J2000)                         | –69°19′53″.9 ± 0″.2  |
| Parameters for partially coherent analysis               |  |
| Braking Index, $n$                                       | 2.140(9)   |
| Glitch Epoch (MJD)                                       | 51342(24)  |
| $\Delta\dot{\nu}/\dot{\nu}$ ( $10^{-4}$ )                | 1.5(1)   |
| Parameters for phase-coherent analysis                   |  |
| Epoch (Modified Julian Day)                              | 51197.0  |
| $\nu$ (Hz) <sup>b</sup>                                  | 19.80244383176(2)  |
| $\dot{\nu}$ ( $10^{-10}$ s <sup>-2</sup> ) <sup>b</sup>  | –1.878039597(8)  |
| $\ddot{\nu}$ ( $10^{-21}$ s <sup>-3</sup> ) <sup>b</sup> | 3.752027(2)  |
| Braking Index, $n^c$                                     | 2.11(6)  |
| Glitch Epoch (MJD)                                       | 51335(12)  |
| $\Delta\nu/\nu$ ( $10^{-9}$ ) <sup>b</sup>               | 1.4(2)   |
| $\Delta\dot{\nu}/\dot{\nu}$ ( $10^{-4}$ ) <sup>b</sup>   | 1.33(2)  |

<sup>a</sup>Position fit from a grid search by minimizing the phase residuals in a phase-coherent analysis, see §3.3.

<sup>b</sup>Quoted uncertainties are formal uncertainties as reported by TEMPO.

<sup>c</sup>Uncertainty determined from variation in  $n$  as higher order derivatives are fitted, as explained in §3.2.

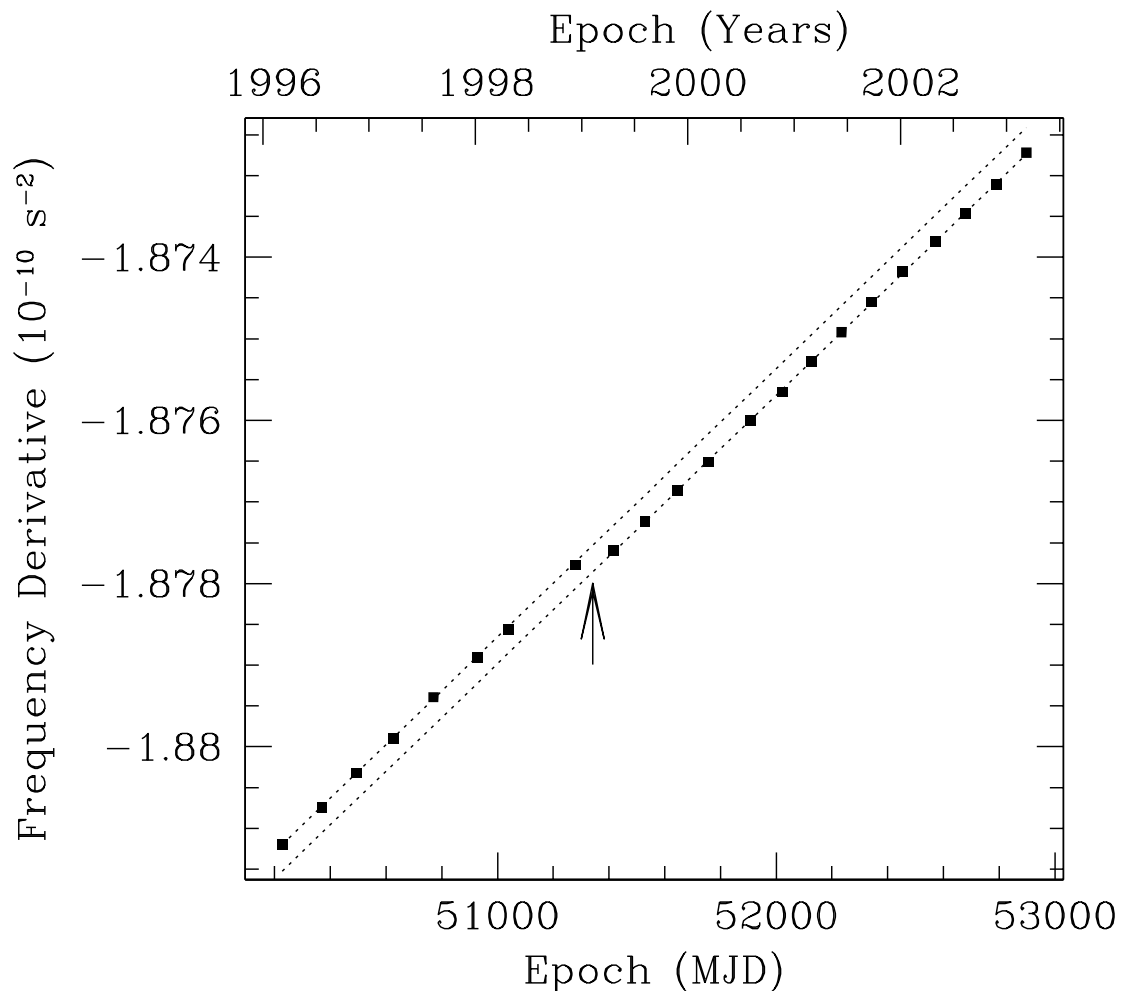


Fig. 1.— Measurements of  $\dot{\nu}$ , the slope is  $\ddot{\nu}$ . The glitch occurring near MJD 51342 is shown with an arrow. The pre-glitch value is  $\ddot{\nu} = (3.81 \pm 0.03) \times 10^{-21} \text{ s}^{-3}$  implying  $n = 2.315 \pm 0.016$ , while the post-glitch value is  $\ddot{\nu} = (3.81 \pm 0.01) \times 10^{-21} \text{ s}^{-3}$  implying  $n = 2.144 \pm 0.007$ . The average of pre- and post-glitch  $n$  is  $2.140 \pm 0.009$ . Measurement uncertainties are smaller than the points and are omitted.

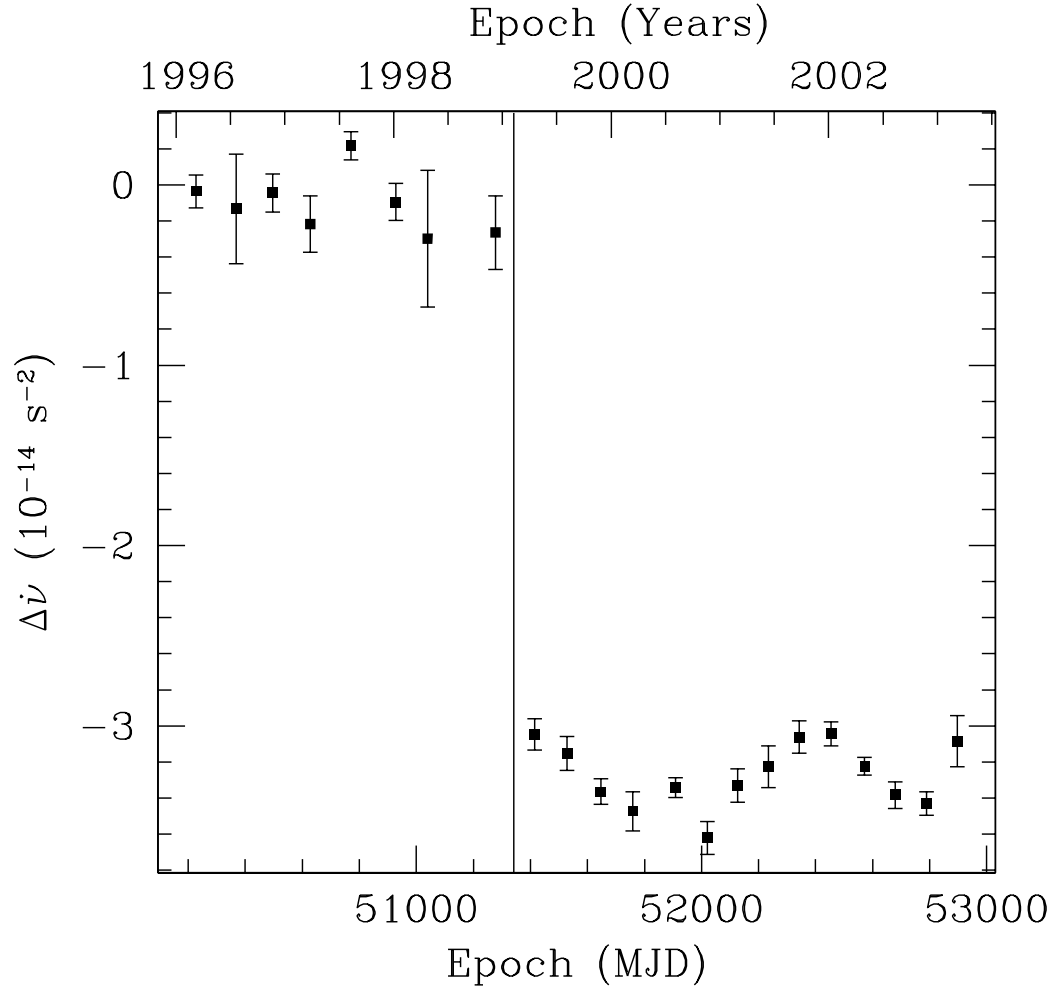


Fig. 2.— Measurements of  $\dot{\nu}$  with the pre-glitch slope (ie.  $\ddot{\nu}$ ) subtracted. The value of  $\Delta\dot{\nu}/\dot{\nu} \sim (1.5 \pm 0.1) \times 10^{-4}$  is in agreement with the value obtained from a phase-coherent analysis. The vertical line indicates the approximate glitch epoch, MJD 51342. The trend in the post-glitch data is attributable to timing noise.

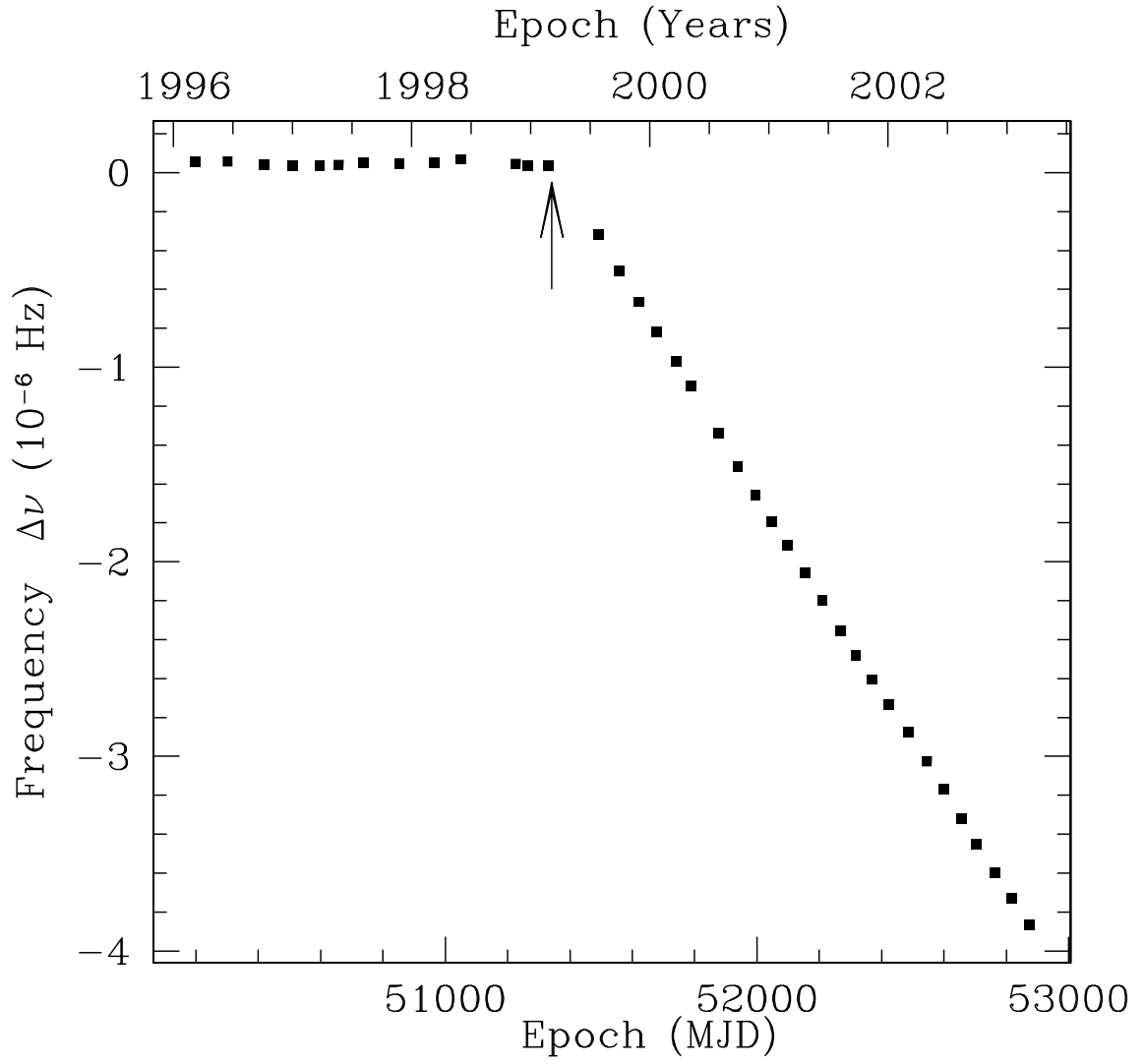


Fig. 3.— Measurements of  $\nu$ , with the pre-glitch trend removed. The arrow marks the glitch epoch, MJD 51342. Uncertainties are smaller than the points.



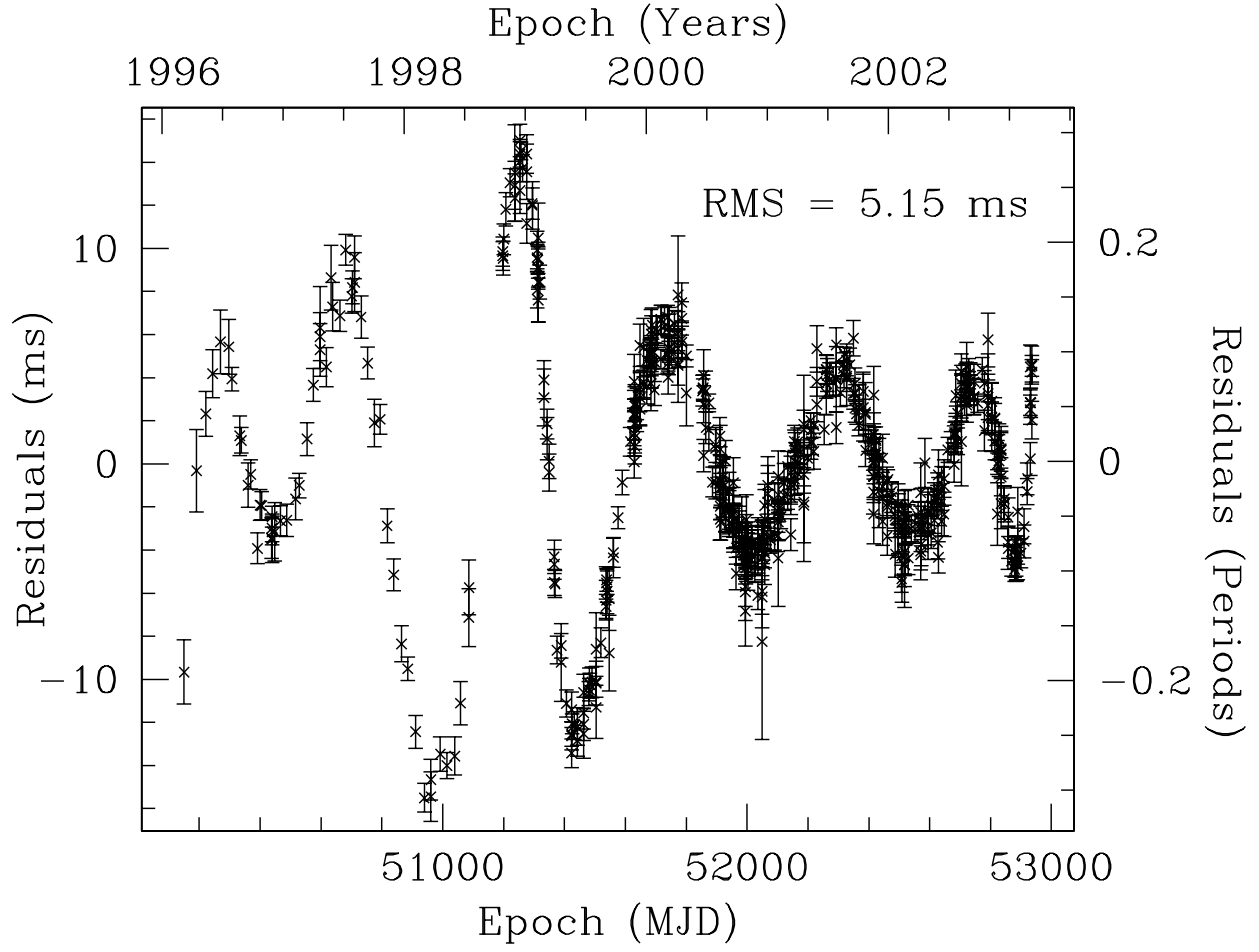


Fig. 4.— Residuals for PSR B0540–69 with  $\nu$  and 11 frequency derivatives – and no glitch – fitted. This was the minimum number of derivatives needed to connect the data, i.e. yield residuals having amplitude less than 0.5 P.

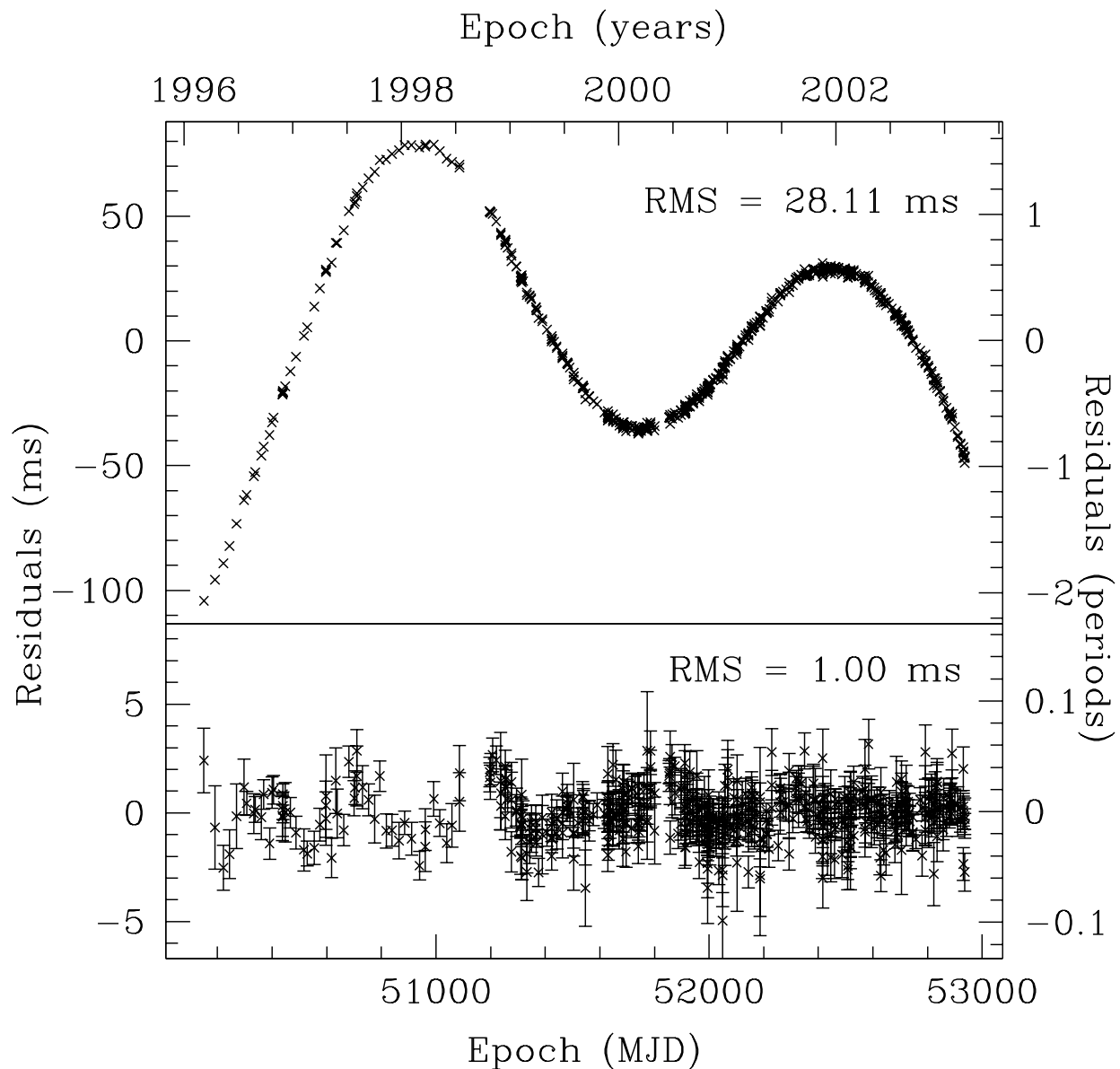


Fig. 5.— Timing residuals for PSR B0540–69. Top panel shows residuals with three glitch parameters and two frequency derivatives fitted. This fit yields a value of  $n = 2.11 \pm 0.06$ . Bottom panel shows residuals with 12 parameters total fitted, for comparison with Figure 4.

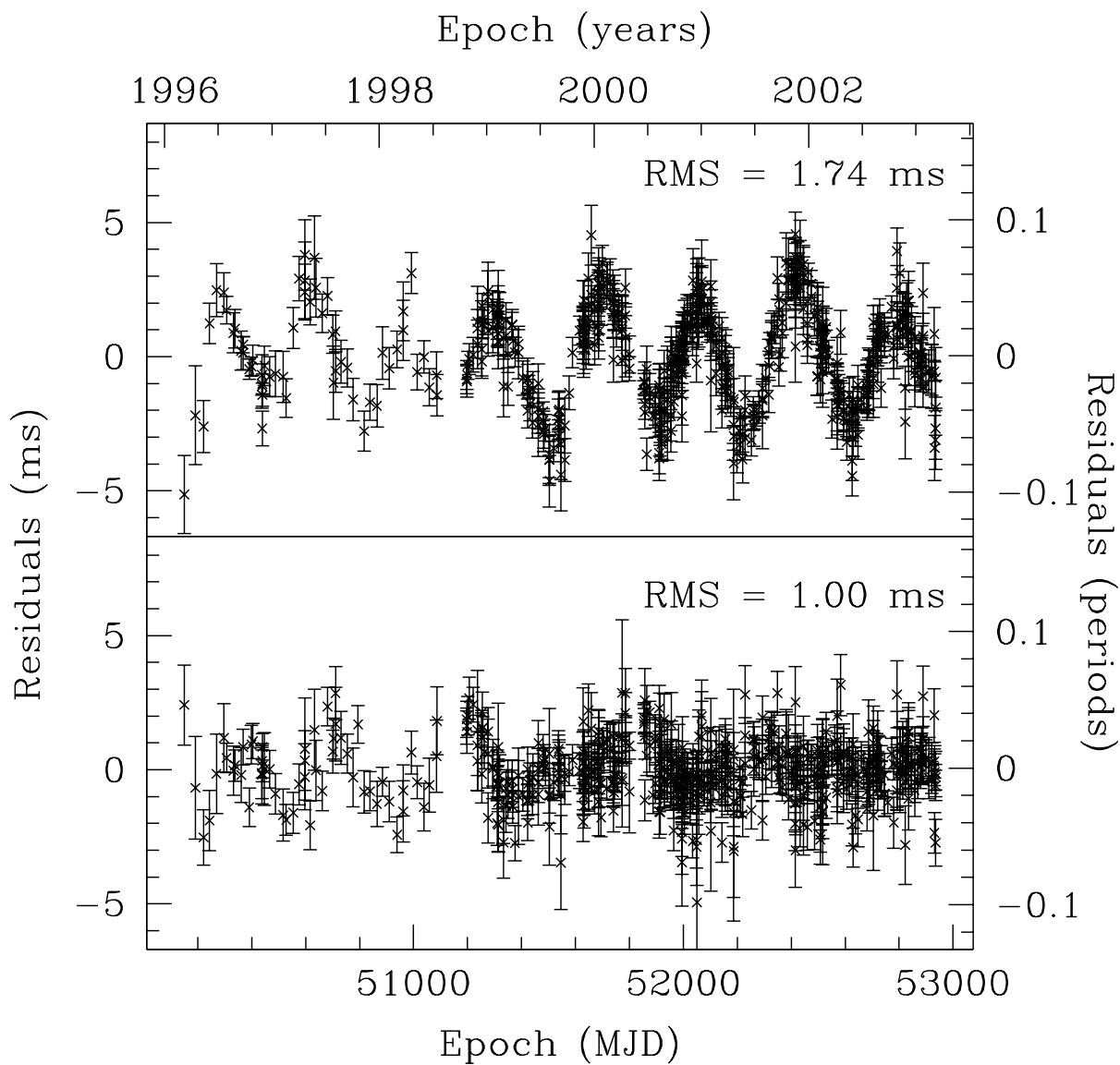


Fig. 6.— RMS residuals for the *Chandra* position (top) and the best-fit position of PSR B0540–69 (bottom). Both sets of residuals have had  $\nu$  and 8 frequency derivatives fitted; removing higher order derivatives does not improve either fit significantly.